

# Evaluating False Alarm and Missing Attacks in CAN IDS

Nirab Hossain

*Department of Applied Mathematics  
University of Colorado Boulder  
Boulder, CO 80309, USA  
nirab.hossain@colorado.edu*

Pablo Moriano

*Computer Science and Mathematics Division  
Oak Ridge National Laboratory  
Oak Ridge, TN 37830, USA  
morianao@ornl.gov*

**Abstract**—Modern vehicles rely on electronic control units (ECUs) interconnected through the Controller Area Network (CAN), making in-vehicle communication a critical security concern. Machine learning (ML)-based intrusion detection systems (IDS) are increasingly deployed to protect CAN traffic, yet their robustness against adversarial manipulation remains largely unexplored. We present a systematic adversarial evaluation of CAN IDS using the ROAD dataset, comparing four shallow learning models with a deep neural network-based detector. Using protocol-compliant, payload-level perturbations generated via FGSM, BIM and PGD, we evaluate adversarial effects on both benign and malicious CAN frames. While all models achieve strong baseline performance under benign conditions, adversarial perturbations reveal substantial vulnerabilities. Although shallow and deep models are robust to false-alarm induction, with the deep neural network (DNN) performing best on benign traffic, all architectures suffer significant increases in missed attacks. Notably, under gradient-based attacks, the shallow model extra trees (ET) demonstrates improved robustness to missed-attack induction compared to the other models. Our results demonstrate that adversarial manipulation can simultaneously trigger false alarms and evade detection, underscoring the need for adversarial robustness evaluation in safety-critical automotive IDS.

**Index Terms**—CPS Security, Intrusion Detection, Controller Area Networks, Machine Learning Security, Adversarial Machine Learning.

## I. INTRODUCTION

Modern vehicles rely on numerous electronic control units (ECUs) to coordinate functions ranging from powertrain and braking to steering and body control [1]. Communication among these components is predominantly supported by the Controller Area Network (CAN), which remains the most widely deployed in-vehicle communication protocol in production vehicles [2]. Designed decades ago for reliable message exchange in closed automotive environments [1], [2], CAN has persisted across vehicle generations due to its simplicity, low cost, and strong backward compatibility [1], [2]. Although higher-bandwidth alternatives such as automotive Ethernet are increasingly introduced [3], CAN continues to underpin many safety-critical subsystems and is unlikely to be phased out in the near term [2], [4]. As a result, understanding CAN’s properties and limitations remains essential for assessing the reliability and security of modern automotive systems.

Despite its widespread adoption, CAN was not designed

with security as a primary objective [1], [2], [4], [5]. It lacks fundamental protection mechanisms such as authentication, encryption, and source verification, operating under the assumption of a trusted in-vehicle environment [5]. As vehicles have become increasingly connected through wireless interfaces, diagnostic ports, and external services, this assumption no longer holds [6], [7]. Prior work has shown that adversaries with CAN-bus access can inject, modify, or replay messages, enabling attacks that affect both vehicle functionality and safety [6]. These attacks can impact critical systems such as braking, steering, and powertrain control, with consequences ranging from denial of service to loss of driver control [6], [8]. Consequently, the combination of protocol-level trust assumptions and safety-critical traffic has made in-vehicle networks an attractive target for high-impact exploits.

To mitigate these risks, intrusion detection systems (IDS) have been widely proposed for CAN-based networks [2]. Early approaches relied on rule-based or signature-driven techniques that detect known attack patterns with low computational overhead [9], [10], but they struggle to generalize to unseen attacks and require frequent updates. To address these limitations, machine learning (ML)-based IDS have gained prominence by leveraging statistical patterns and learned representations of normal CAN traffic [2]. Initial solutions employed shallow models such as decision trees, support vector machines, and ensemble methods [11], offering interpretability and modest training requirements. More recent work has adopted deep learning (DL) architectures, including convolutional and recurrent models, to capture temporal dependencies and complex correlations across CAN messages [12], [13]. These DL-based approaches have demonstrated strong detection performance in controlled settings, accelerating their adoption in automotive IDS research.

Despite their empirical success, ML-based IDS introduce vulnerabilities that manifest in distinct and equally problematic failure modes [14], [15]. One failure mode involves false alarms, where benign CAN traffic is misclassified as malicious due to subtle input perturbations [16]. In safety-critical systems, excessive false positives can degrade reliability, trigger unnecessary mitigation actions, and erode trust in the IDS. A complementary failure mode arises when adversarial manipulations cause false negatives, allowing malicious CAN

messages to evade detection [17]. Unlike rule-based systems, learned decision boundaries can be intentionally influenced through carefully crafted, protocol-compliant inputs [18], enabling attackers to induce either outcome without violating CAN specifications. These dual failure modes expose fundamental robustness challenges for ML-based CAN IDS under realistic adversarial conditions.

Building on these observations, this work evaluates the adversarial robustness of CAN-bus IDS by both separately and jointly examining false alarms and missed attacks as coupled adversarial failure modes that determine IDS reliability under attack [14]. We focus on protocol-compliant, payload-level manipulations that preserve CAN frame validity while influencing IDS decisions at inference time [16]. Unlike prior studies that consider false alarms or evasion in isolation [16], [17], we adopt a unified evaluation framework applied consistently across representative ML-based IDS families. By grounding the analysis in realistic CAN attack scenarios from the ROAD dataset [19], our study enables a more faithful assessment of adversarial effects under practical traffic and attacker conditions. This paper makes the following contributions:

- We present a unified adversarial evaluation of CAN-bus IDS that both separately and jointly considers false alarms (false positives) and missed attacks (false negatives) as coupled failure modes.
- We design and apply protocol-compliant, payload-level adversarial perturbations and evaluate them against realistic CAN attack scenarios from the ROAD dataset.
- We conduct a comparative analysis across representative ML-based IDS families, including shallow and DL models, to characterize how architectural choices influence adversarial robustness.
- We illustrate adversarial failure modes that are not captured when IDS performance is assessed only on clean test data.
- To support reproducibility and further research, we make our implementation, experimental pipeline, and evaluation code publicly available at [20].

## II. RELATED WORKS

IDS on the automotive CAN bus has been widely studied, with increasing emphasis on ML-based IDS. Early approaches relied on statistical or rule-based techniques to detect deviations from expected CAN traffic patterns [9], [10], [21]. While computationally efficient, these methods are typically limited to known attack signatures and struggle to generalize to unseen behaviors. Consequently, recent research has shifted toward data-driven IDS models. Sun *et al.* [22], for example, demonstrated that hybrid deep architectures combining CNNs and LSTMs with attention mechanisms can capture temporal dependencies in CAN traffic for anomaly detection. Beyond this, a broad range of DL architectures, including CNNs and GRUs, as well as ensemble methods, have been explored. In parallel, unsupervised techniques such as clustering and PCA, together with classical classifiers including SVMs, k-NN, and decision trees, have been proposed for CAN anomaly detection [4], [11]. Wu *et al.* [2] provide a comprehensive

survey of in-vehicle IDS approaches, highlighting the diversity of modeling choices and evaluation practices in the field.

At the same time, adversarial machine learning (AML) has emerged as a critical concern for security-sensitive ML systems. Seminal work by Goodfellow *et al.* [18] and Carlini and Wagner [23] established that carefully crafted gradient-based perturbations can cause neural networks to misclassify inputs with high confidence. In the broader cybersecurity domain, He *et al.* [15] reviewed adversarial attacks on ML-based IDS and showed their effectiveness across a wide range of settings. However, within the automotive domain, adversarial research has largely focused on perception and autonomous driving tasks, with comparatively limited attention given to the robustness of in-vehicle IDS [24].

A smaller body of work has begun to address adversarial attacks targeting automotive IDS directly. Pacheco *et al.* [25] applied FGSM, JSMA, and CW attacks to IDS, primarily analyzing adversarially induced false negatives. Zenden *et al.* [26] evaluated FGSM-based attacks on CAN IDS, examining transferability, adversarial training, and standard performance metrics such as FPR and FNR, but did not consider stronger multi-step attacks or provide a detailed analysis of failure modes under protocol-constrained perturbations. Longari *et al.* [17] proposed an online, oracle-guided evasion strategy that perturbs CAN payload bits in attacks such as Drop, Fuzzy, Replay, and Seamless Change, studying IDS robustness under different attacker knowledge assumptions. More recently, Aloraini *et al.* [16] investigated adversarial attacks on ML-based CAN IDS by applying FGSM, BIM, PGD, and decision-tree-based attacks to benign traffic, showing that adversarial perturbations can reliably induce false alarms across multiple models.

In contrast to prior work, our study evaluates both shallow and DL-based CAN IDS using a unified adversarial framework grounded in the comprehensive ROAD dataset. By applying protocol-compliant adversarial attacks, including FGSM, BIM, and PGD, we provide a more architecture-sensitive and realistic assessment of IDS robustness. Crucially, we examine adversarially induced false alarms and missed attacks both in isolation and in combination, enabling a more complete characterization of IDS reliability in safety-critical in-vehicle network settings.

Dataset choice is central to IDS evaluation. While several CAN intrusion datasets exist, many are limited in duration or attack diversity. For example, the Car-Hacking dataset contains only a small number of attack types and short driving traces. In contrast, the ROAD dataset [19] offers over 3.5 hours of real vehicle CAN traffic, comprising 12 benign captures and 33 attack captures, including random fuzzing floods, targeted fabrication attacks, and ECU masquerade scenarios. We therefore adopt ROAD to ensure that our evaluation reflects diverse driving conditions and adversarial behaviors.

## III. MATERIALS AND METHODS

### A. CAN

CAN is the primary in-vehicle communication bus used to interconnect multiple ECUs [27]. It employs a broadcast,

message-based protocol in which each frame, illustrated in Fig. 1, consists of an identifier (ID), a data length code (DLC), up to eight data bytes, and error-checking fields. Medium access is governed by priority-based arbitration, where frames with lower numerical IDs are granted access to the bus before higher-priority messages.

SoF	ID	DLC	Data	CRC	ACK	EoF
-----	----	-----	------	-----	-----	-----

Fig. 1. CAN data frame structure.

In classical CAN, the *payload* corresponds to the raw data field comprising up to eight bytes (D0–D7), represented as hexadecimal values in CAN logs. Those data bytes are treated directly as numerical features derived from observed CAN traffic. Under this representation, each frame contributes its eight data bytes as independent features, enabling both benign and malicious behaviors to be analyzed at the level of raw payload values.

Within our methodology, adversarial manipulation is restricted to the payload bytes. This design choice reflects an attack surface in which an adversary alters message contents without violating protocol structure or disrupting normal bus arbitration. Although CAN provides efficient and reliable real-time communication, it lacks fundamental security mechanisms such as authentication and encryption. Consequently, a compromised ECU can inject, modify, or replay messages that appear legitimate to other nodes on the network. These limitations have motivated extensive research on intrusion detection systems for CAN networks, including both shallow and DL-based unsupervised approaches [2], [5], [21], [27].

### B. IDS Architecture

Our IDS operates at the frame level and uses supervised ML models to classify each CAN message independently based on its payload byte features. The classification is performed without relying on sliding windows or temporal aggregation, with feature preparation conducted as described in III-E. This design isolates per-frame decision behavior and enables a controlled analysis of model responses under benign and adversarial conditions.

We consider five classifiers: decision tree (DT), random forest (RF), extra trees (ET), XGBoost (XGB), and a deep neural network (DNN). DT provides simple hierarchical decision rules but is sensitive to model depth, which can lead to overfitting or underfitting. RF and ET address this limitation by aggregating multiple randomized trees, reducing variance and yielding stronger and more stable baselines. XGB further improves performance through gradient-boosted trees that capture complex feature interactions across payload bytes. The DNN consists of four fully connected hidden layers with 16 neurons each using ReLU activations, followed by a single sigmoid output neuron for binary classification. Following the work by Aloraini *et al.* [16], these models enable a direct comparison between shallow and DL-based IDS approaches under both benign and adversarial evaluation settings.

### C. Threat Model

We assume an external adversary with access to the CAN bus who is capable of injecting fabricated messages while imitating legitimate ECUs, corresponding to a gray-bus attack scenario. For adversarial evaluation, we further assume that the attacker has white-box knowledge of the IDS, which enables the computation of gradient-based adversarial perturbations. The adversary's primary objective is to exploit false positives by manipulating benign frames so that they are flagged as malicious, thereby disrupting normal vehicle operation and gradually eroding trust in the IDS as well as to evade detection by the IDS while inducing unauthorized effects, such as spoofing sensor readings or suppressing alerts. This threat model captures both false-alarms and evasion-oriented adversarial objectives relevant to safety-critical CAN environments.

### D. Dataset

We use the ROAD CAN IDS dataset [19], a high-fidelity collection of CAN bus traffic that includes both normal driving behavior and a diverse set of verified attack scenarios. The dataset comprises over 3.5 hours of CAN traffic collected from a real vehicle under dynamometer testing conditions, including 12 ambient (benign) captures and 33 attack captures. The attack scenarios span a range of difficulty, from easily detectable behaviors to more stealthy manipulations. In particular, ROAD includes random fuzzing floods as well as targeted fabrication attacks that inject malicious data for specific CAN IDs. All CAN frames are timestamped and labeled, with the aid of accompanying metadata, as either *normal* or as a specific attack type, enabling supervised training and evaluation of intrusion detection models. The evaluated attacks include fuzzing attacks (FA) and fabrication attacks such as max engine coolant temperature (MECTA), max speedometer (MSA), reverse light off (RLOFFA), reverse light on (RLONA), and correlated signal (CSA) attacks. Table I summarizes the types of attacks used in this study.

TABLE I  
STATISTICAL BREAKDOWN OF ATTACKS IN THE ROAD DATASET.

Attack Type	Benign	Malicious	Total
FA	87,907	1,061	88,968
MECTA	57,932	88	58,020
MSA	520,216	17,221	537,437
RLOFFA	180,357	10,605	190,962
RLONA	480,021	15,195	495,216
CSA	175,412	5,493	180,905
<b>Total</b>	<b>1,501,845</b>	<b>49,663</b>	<b>1,551,508</b>

### E. Preprocessing

CAN logs were parsed using a custom Python script that extracted the data field payload from each frame. The data field was padded with leading zeros to ensure a fixed length of 16 hexadecimal characters corresponding to eight bytes. The payload bytes (D0–D7) were then extracted from the hexadecimal string and converted to decimal values.

Labels were assigned by matching each frame against the known injected attack data, with frames labeled as benign (0) or malicious (1). The resulting structured dataset was stored

in CSV format. Each frame was treated independently during preprocessing, using payload bytes (D0–D7) as features and the binary flag as the label, without incorporating temporal context or aggregation.

#### F. Domain Constraints

To ensure that adversarial examples remain valid CAN frames, we enforce protocol-level domain constraints during attack generation. Prior work has noted that many AML studies overlook such constraints in networked systems, resulting in perturbations that may be effective in theory but invalid on the wire [4], [24]. In classical CAN, each frame is defined by an ID, a DLC, and up to eight data bytes. In practice, ECUs transmit and accept only a fixed set of IDs configured by the manufacturer, and DLC values are determined by firmware and hardware constraints. Modifying these fields would therefore produce frames that are trivially rejected or never generated in real vehicles.

Under our threat model, the adversary operates exclusively on the payload bytes of existing frames. The CAN ID and DLC fields are held fixed to preserve message routing and length, while the eight data bytes (D0–D7) constitute the only mutable components. Accordingly, perturbations are restricted to payload-byte feature columns, ensuring that gradients are applied only to CAN data bytes.

After each update, perturbed payload values are clipped to the valid CAN byte range [0, 255] and converted back to integer values prior to evaluation. By constraining the attacker in this manner, we emulate a realistic CAN-bus adversary who reuses legitimate IDs and timings while manipulating only the data field. This design choice is consistent with established in-vehicle threat models and recent CAN IDS studies [4], [16], [19], [24].

#### G. Adversarial Attack Methods

To evaluate the robustness of the proposed IDS against adaptive adversaries, we generate adversarial examples using established gradient-based techniques. We leverage the Adversarial Robustness Toolbox (ART) [28] to craft attacks that introduce subtle, targeted manipulations of CAN payload bytes with the goal of inducing misclassification. An overview of the adversarial workflow is illustrated in Fig. 2. The following attack methods are considered in our experiments:

- **FGSM** [18]: A single-step white-box attack that computes the gradient of the IDS loss with respect to the input features and perturbs the input in the direction of the sign of the gradient. We apply FGSM using a small perturbation budget  $\epsilon$ , adding an  $\epsilon$ -scaled sign of the gradient to each payload feature. This produces adversarial CAN frames with minimal changes to data values that can nonetheless cause the IDS to misclassify individual frames.
- **BIM** [29]: An iterative extension of FGSM, also referred to as I-FGSM. BIM applies multiple small gradient-based updates, each scaled by a fraction of  $\epsilon$ , while clipping the perturbed input after every step to preserve validity. This iterative refinement results in stronger adversarial examples that remain within the allowed perturbation bounds.

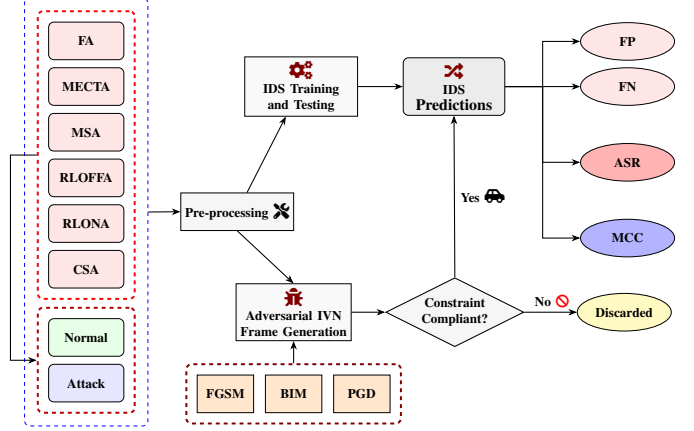


Fig. 2. Workflow for IDS training, adversarial IVN frame generation, and evaluation of benign and adversarial predictions with FN, FP, and MCC.

- **PGD** [30]: A multi-step attack that generalizes BIM by incorporating random initialization within the allowed perturbation region. PGD performs a sequence of gradient-based updates and projects the perturbed input back into the  $\epsilon$ -ball around the original sample after each step. Often regarded as a strong first-order adversary, PGD approximates a worst-case attack against a given model by generating minimally perturbed CAN frames that maximize prediction error under full IDS knowledge.

In this work, FGSM, BIM, and PGD attacks are generated using a differentiable DNN surrogate and the resulting adversarial samples are then reused to evaluate the robustness of shallow models in a transfer-based setting under identical protocol-constrained perturbations consistent with Pacheco *et al.* [25]. Also, we evaluate IDS robustness under bounded payload perturbations applied to frames labeled benign or malicious in the ROAD dataset without claiming semantic or physical class preservation. Following the use of  $L_\infty$ -bounded perturbations in Carlini *et al.* [23], the perturbation budget  $\epsilon$  enforces a per-byte bound with  $\epsilon \in \{1, 5\}$  in our experiments, yielding small, valid-range numerical changes that constrain perturbation magnitude for both benign and attack data, but do not guarantee semantic invariance, and thus this setup enables the evaluation of false alarms and missed detections under adversarial conditions.

#### H. Evaluation Metrics

We evaluate adversarial effectiveness and classifier performance using two complementary metrics: the attack success rate (ASR) [31] and the Matthews correlation coefficient (MCC) [32]. ASR quantifies how often crafted adversarial samples successfully induce misclassification by the IDS. Formally, let  $N_{\text{adv}}$  denote the number of adversarially perturbed samples and  $N_{\text{succ}}$  the number of those samples that are misclassified by the IDS. ASR is then defined as  $\text{ASR} = \frac{N_{\text{succ}}}{N_{\text{adv}}}$ .

In the IDS setting considered here, ASR captures two distinct adversarial objectives: inducing benign frames to be flagged as malicious (false positives) and causing malicious

frames to be misclassified as normal (false negatives). Expressed in terms of confusion-matrix entries, the ASR for benign inputs, corresponding to adversarially induced false alarms is  $\text{ASR}_{[FP]}$ , while for malicious inputs, it is  $\text{ASR}_{[FN]}$  expressed as

$$\text{ASR}_{[FP]} = \frac{\text{FP}_{[adv]}}{\text{TN}_{[adv]} + \text{FP}_{[adv]}}, \quad \text{ASR}_{[FN]} = \frac{\text{FN}_{[adv]}}{\text{TP}_{[adv]} + \text{FN}_{[adv]}}$$

respectively. Although these expressions resemble the standard false negative rate and false positive rate, they are computed exclusively over adversarially perturbed samples. As such, they directly quantify attacker success in terms of missed attacks and induced false alarms. Higher ASR values indicate more effective adversarial attacks and reduced IDS robustness.

In addition to ASR, we report MCC to assess overall classification performance under class imbalance. FP and FN are computed from evaluations on benign-only and malicious-only subsets, respectively, to isolate false-alarm and miss-detection behavior. In contrast, MCC is evaluated on the full test set containing both benign and malicious frames, where joint classification performance under class imbalance can be meaningfully assessed. The ROAD dataset contains approximately 1.5 million benign frames and 50 thousand malicious frames, resulting in a strongly imbalanced class distribution of about 3.2% malicious traffic [19]. Under such conditions, commonly used metrics such as the F1 score can overestimate performance by favoring the majority class [16]. MCC is well suited to this setting because it incorporates all four confusion-matrix components and provides a balanced summary of binary classification quality. Given the counts TP, TN, FP, and FN, MCC is defined as

$$\text{MCC} = \frac{\text{TP} \cdot \text{TN} - \text{FP} \cdot \text{FN}}{\sqrt{(\text{TP} + \text{FP})(\text{TP} + \text{FN})(\text{TN} + \text{FP})(\text{TN} + \text{FN})}}.$$

MCC ranges from  $-1$  (total disagreement) to  $0$  (no better than random) and up to  $+1$  (perfect prediction). We report MCC alongside FP/FN counts and their respective ASR of benign-only and malicious-only subsets to provide a robust view of IDS performance that penalizes both false alarms and missed-detections within a single scalar measure.

## IV. RESULTS

### A. Overview of Evaluation

Table I summarizes the data used for training and evaluation. The IDS classifiers are trained on a merged dataset comprising six subsets including a fuzzing attack and five fabrication attacks for a total of 1,551,508 samples after preprocessing. This dataset contains 1,501,845 benign samples and 49,663 malicious samples. We apply a 70/30 train–test split, resulting in 1,086,055 samples for training and 465,453 samples for testing, with class proportions preserved under random shuffling (96.8% benign and 3.2% malicious).

Table II reports the baseline performance of each IDS on the 30% test set, including false positives (FPs), false negatives (FNs), and MCC values. The results indicate that shallow models achieve strong nominal detection performance, with MCC values close to 0.91. In contrast, the DNN attains a slightly lower MCC (approximately 0.85), exhibiting fewer false positives but substantially more false negatives, which

TABLE II  
PERFORMANCE METRICS ON TEST SAMPLES UNDER BENIGN SETTINGS.

Model	Benign	Malicious	FP	FN	MCC
DT			941	1,668	0.908
RF			951	1,659	0.908
ET	450,554	14,899	929	1,683	0.907
XGB			966	1,638	0.908
DNN			384	3,781	0.845

TABLE III  
COMPARATIVE ANALYSIS – FA.

Model	Benign			Attack	Adversarial					
	$\epsilon$	FP	FN	MCC	$\epsilon$	FP	ASR	FN	ASR	MCC
DT	22	0	0.99	FGSM	1	67	0.001	0	0.0	0.838
	22	0	0.99	FGSM	5	67	0.001	0	0.0	0.789
	22	0	0.99	BIM	1	67	0.001	0	0.0	0.833
	22	0	0.99	BIM	5	67	0.001	0	0.0	0.833
	22	0	0.99	PGD	1	188	0.003	84	0.134	0.777
	22	0	0.99	PGD	5	294	0.005	192	0.306	0.638
RF	20	0	0.989	FGSM	1	8	0.0	0	0.0	0.998
	20	0	0.989	FGSM	5	8	0.0	0	0.0	0.994
	20	0	0.989	BIM	1	8	0.0	0	0.0	0.998
	20	0	0.989	BIM	5	8	0.0	0	0.0	0.998
	20	0	0.989	PGD	1	11	0.0	84	0.134	0.978
	20	0	0.989	PGD	5	38	0.001	207	0.33	0.812
ET	18	0	0.992	FGSM	1	8	0.0	0	0.0	1.0
	18	0	0.992	FGSM	5	8	0.0	0	0.0	1.0
	18	0	0.992	BIM	1	8	0.0	0	0.0	1.0
	18	0	0.992	BIM	5	8	0.0	0	0.0	1.0
	18	0	0.992	PGD	1	4	0.0	0	0.0	1.0
	18	0	0.992	PGD	5	31	0.001	0	0.0	0.995
XGB	22	0	0.99	FGSM	1	69	0.001	0	0.0	0.994
	22	0	0.99	FGSM	5	69	0.001	0	0.0	0.948
	22	0	0.99	BIM	1	69	0.001	0	0.0	0.983
	22	0	0.99	BIM	5	69	0.001	0	0.0	0.983
	22	0	0.99	PGD	1	34	0.001	312	0.499	0.898
	22	0	0.99	PGD	5	90	0.001	321	0.512	0.742
DNN	19	24	0.978	FGSM	1	6	0.0	24	0.038	0.992
	19	24	0.978	FGSM	5	6	0.0	24	0.038	0.803
	19	24	0.978	BIM	1	6	0.0	24	0.038	0.992
	19	24	0.978	BIM	5	6	0.0	24	0.038	0.992
	19	24	0.978	PGD	1	6	0.0	26	0.042	0.99
	19	24	0.978	PGD	5	43	0.001	26	0.041	0.99

suggests a more conservative decision boundary favoring the benign class. This baseline evaluation establishes that any performance degradation observed under adversarial perturbations can be attributed to the attacks themselves rather than to inadequate nominal IDS performance.

Table III through Table VII present results for adversarial evaluation, reporting FPs, FNs, ASR, and MCC across all models and attack scenarios. For the CSA subset, shown in Table VIII, no false negatives are produced; accordingly, results for this case are reported using F1 scores since MCC is zero when false negatives are not produced.

### B. Benign Performance and False-Alarm Robustness

Across all attack methods (FGSM, BIM, and PGD) and perturbation budgets ( $\epsilon = 1, 5$ ), the IDS models generally maintain stable benign classification performance, as reflected by the MCC values that remain close to their nominal baselines. With the exception of PGD at  $\epsilon = 5$ , which leads to noticeable degradation, shallow models largely preserve their ability to correctly classify benign traffic under adversarial perturbations. On the other hand, the DNN exhibits significantly lower ASR accurately capturing benign frames than other models in benign settings under adversarial conditions.

TABLE IV  
COMPARATIVE ANALYSIS – MECTA.

Model	Benign			Attack	$\epsilon$	Adversarial				
	FP	FN	MCC			FP	ASR	FN	ASR	MCC
DT	17	26	0.748	FGSM	1	14	0.0	4	0.667	-0.0
	17	26	0.748	FGSM	5	14	0.0	4	0.667	-0.0
	17	26	0.748	BIM	1	14	0.0	4	0.667	-0.0
	17	26	0.748	BIM	5	14	0.0	4	0.667	-0.0
	17	26	0.748	PGD	1	159	0.004	3	0.5	0.051
	17	26	0.748	PGD	5	279	0.007	4	0.667	-0.001
RF	16	27	0.748	FGSM	1	13	0.0	4	0.667	0.0
	16	27	0.748	FGSM	5	13	0.0	4	0.667	0.0
	16	27	0.748	BIM	1	13	0.0	4	0.667	0.0
	16	27	0.748	BIM	5	13	0.0	4	0.667	0.0
	16	27	0.748	PGD	1	26	0.001	3	0.5	0.085
	16	27	0.748	PGD	5	11	0.0	4	0.667	-0.0
ET	16	27	0.733	FGSM	1	13	0.0	4	0.667	-0.0
	16	27	0.733	FGSM	5	13	0.0	4	0.667	0.0
	16	27	0.733	BIM	1	13	0.0	4	0.667	-0.0
	16	27	0.733	BIM	5	13	0.0	4	0.667	-0.0
	16	27	0.733	PGD	1	24	0.001	3	0.5	0.091
	16	27	0.733	PGD	5	50	0.001	4	0.667	-0.0
XGB	16	27	0.733	FGSM	1	13	0.0	4	0.667	-0.0
	16	27	0.733	FGSM	5	13	0.0	4	0.667	-0.0
	16	27	0.733	BIM	1	13	0.0	4	0.667	-0.0
	16	27	0.733	BIM	5	13	0.0	4	0.667	-0.0
	16	27	0.733	PGD	1	13	0.0	6	1.0	-0.0
	16	27	0.733	PGD	5	60	0.001	5	0.833	-0.0
DNN	0	88	-0.0	FGSM	1	0	0.0	6	1.0	0.0
	0	88	-0.0	FGSM	5	0	0.0	6	1.0	-0.001
	0	88	-0.0	BIM	1	0	0.0	6	1.0	0.0
	0	88	-0.0	BIM	5	0	0.0	6	1.0	0.0
	0	88	-0.0	PGD	1	7	0.0	6	1.0	0.0
	0	88	-0.0	PGD	5	746	0.018	6	1.0	-0.001

TABLE V  
COMPARATIVE ANALYSIS – MSA.

Model	Benign			Attack	$\epsilon$	Adversarial				
	FP	FN	MCC			FP	ASR	FN	ASR	MCC
DT	1031	570	0.962	FGSM	1	1002	0.003	13	0.001	0.86
	1031	570	0.962	FGSM	5	1002	0.003	13	0.001	0.838
	1031	570	0.962	BIM	1	1002	0.003	13	0.001	0.872
	1031	570	0.962	BIM	5	1002	0.003	13	0.001	0.879
	1031	570	0.962	PGD	1	1124	0.003	3602	0.243	0.773
	1031	570	0.962	PGD	5	2830	0.008	6690	0.451	0.638
RF	989	486	0.96	FGSM	1	961	0.003	24	0.002	0.858
	989	486	0.96	FGSM	5	961	0.003	24	0.002	0.855
	989	486	0.96	BIM	1	961	0.003	24	0.002	0.851
	989	486	0.96	BIM	5	961	0.003	24	0.002	0.858
	989	486	0.96	PGD	1	632	0.002	4418	0.298	0.763
	989	486	0.96	PGD	5	751	0.002	7835	0.528	0.66
ET	1026	584	0.961	FGSM	1	998	0.003	276	0.019	0.855
	1026	584	0.961	FGSM	5	998	0.003	112	0.008	0.854
	1026	584	0.961	BIM	1	998	0.003	276	0.019	0.859
	1026	584	0.961	BIM	5	998	0.003	112	0.008	0.867
	1026	584	0.961	PGD	1	165	0.0	2217	0.149	0.885
	1026	584	0.961	PGD	5	283	0.001	2851	0.192	0.887
XGB	1007	442	0.956	FGSM	1	980	0.003	13	0.001	0.858
	1007	442	0.956	FGSM	5	980	0.003	13	0.001	0.833
	1007	442	0.956	BIM	1	980	0.003	13	0.001	0.863
	1007	442	0.956	BIM	5	980	0.003	13	0.001	0.873
	1007	442	0.956	PGD	1	249	0.001	7360	0.496	0.648
	1007	442	0.956	PGD	5	1754	0.005	7468	0.503	0.63
DNN	237	4226	0.855	FGSM	1	183	0.001	3152	0.212	0.882
	237	4226	0.855	FGSM	5	183	0.001	3152	0.212	0.783
	237	4226	0.855	BIM	1	183	0.001	3152	0.212	0.882
	237	4226	0.855	BIM	5	183	0.001	3152	0.212	0.882
	237	4226	0.855	PGD	1	182	0.001	3152	0.212	0.882
	237	4226	0.855	PGD	5	1475	0.004	3156	0.213	0.863

This behavior suggests that the DNN demonstrates superior robustness to adversarial perturbations on benign traffic, limiting false-alarm induction compared to shallow models.

#### C. Adversarial Performance and Missed-Attack Vulnerability

Results for adversarial perturbations applied to malicious samples, summarized in Table III through Table VIII, re-

TABLE VI  
COMPARATIVE ANALYSIS – RLOFFA.

Model	Benign			Attack	$\epsilon$	Adversarial				
	FP	FN	MCC			FP	ASR	FN	ASR	MCC
DT	18	4590	0.733	FGSM	1	6	0.0	2799	0.438	0.34
	18	4590	0.733	FGSM	5	6	0.0	2799	0.438	0.401
	18	4590	0.733	BIM	1	6	0.0	2799	0.438	0.349
	18	4590	0.733	BIM	5	6	0.0	2799	0.438	0.35
	18	4590	0.733	PGD	1	535	0.004	5175	0.81	0.188
	18	4590	0.733	PGD	5	492	0.004	6096	0.954	0.129
RF	18	4650	0.738	FGSM	1	6	0.0	2859	0.448	0.443
	18	4650	0.738	FGSM	5	6	0.0	2859	0.448	0.439
	18	4650	0.738	BIM	1	6	0.0	2859	0.448	0.454
	18	4650	0.738	BIM	5	6	0.0	2859	0.448	0.454
	18	4650	0.738	PGD	1	25	0.0	5373	0.841	0.231
	18	4650	0.738	PGD	5	54	0.0	6368	0.997	0.029
ET	18	4590	0.733	FGSM	1	6	0.0	2799	0.438	0.423
	18	4590	0.733	FGSM	5	6	0.0	2799	0.438	0.413
	18	4590	0.733	BIM	1	6	0.0	2799	0.438	0.423
	18	4590	0.733	BIM	5	6	0.0	2799	0.438	0.423
	18	4590	0.733	PGD	1	24	0.0	5354	0.838	0.166
	18	4590	0.733	PGD	5	64	0.001	6365	0.997	0.025
XGB	18	4593	0.742	FGSM	1	6	0.0	2799	0.438	0.45
	18	4593	0.742	FGSM	5	6	0.0	2799	0.438	0.439
	18	4593	0.742	BIM	1	6	0.0	2799	0.438	0.605
	18	4593	0.742	BIM	5	6	0.0	2799	0.438	0.602
	18	4593	0.742	PGD	1	27	0.0	5642	0.883	0.148
	18	4593	0.742	PGD	5	135	0.001	6333	0.992	0.031
DNN	6	6687	0.612	FGSM	1	6	0.0	4566	0.715	0.371
	6	6687	0.612	FGSM	5	0	0.0	4566	0.715	0.153
	6	6687	0.612	BIM	1	6	0.0	4566	0.715	0.372
	6	6687	0.612	BIM	5	0	0.0	4566	0.715	0.372
	6	6687	0.612	PGD	1	3	0.0	4624	0.724	0.394
	6	6687	0.612	PGD	5	72	0.001	5465	0.856	0.318

veal substantial missed-attack vulnerabilities across the evaluated IDS models. Under FGSM, BIM, and PGD attacks on MECTA, the DNN consistently exhibits an attack success rate (ASR) of 1.0, indicating a complete failure to detect adversarially manipulated malicious frames and resulting in non-positive MCC. The shallow models also yield close to

TABLE VIII  
COMPARATIVE ANALYSIS – CSA.

Model	Benign		$\epsilon$	Adversarial		
	F1 Score	FP		F1 Score	FP	ASR
DT	1.000	99	FGSM	1	0.999	137 0.001
	1.000	99	FGSM	5	0.999	137 0.001
	1.000	99	BIM	1	0.999	137 0.001
	1.000	99	BIM	5	0.999	137 0.001
	1.000	99	PGD	1	0.999	214 0.002
	1.000	99	PGD	5	0.998	440 0.004
RF	1.000	97	FGSM	1	1.000	48 0.000
	1.000	97	FGSM	5	1.000	48 0.000
	1.000	97	BIM	1	1.000	48 0.000
	1.000	97	BIM	5	1.000	48 0.000
	1.000	97	PGD	1	1.000	27 0.000
	1.000	97	PGD	5	1.000	65 0.001
ET	1.000	97	FGSM	1	1.000	47 0.000
	1.000	97	FGSM	5	1.000	47 0.000
	1.000	97	BIM	1	1.000	47 0.000
	1.000	97	BIM	5	1.000	47 0.000
	1.000	97	PGD	1	1.000	9 0.000
	1.000	97	PGD	5	1.000	19 0.000
XGB	1.000	115	FGSM	1	0.999	137 0.001
	1.000	115	FGSM	5	0.999	137 0.001
	1.000	115	BIM	1	0.999	137 0.001
	1.000	115	BIM	5	0.999	137 0.001
	1.000	115	PGD	1	1.000	51 0.000
	1.000	115	PGD	5	0.999	191 0.002
DNN	0.999	322	FGSM	1	1.000	69 0.001
	0.999	322	FGSM	5	1.000	69 0.001
	0.999	322	BIM	1	1.000	69 0.001
	0.999	322	BIM	5	1.000	69 0.001
	0.999	322	PGD	1	1.000	59 0.000
	0.999	322	PGD	5	1.000	93 0.001

No FN results for CSA were produced in `csa_fn.csv`.

zero MCC on MECTA, implying performance no better than random guessing. Similarly, the shallow models suffer severe degradation for PGD at both perturbations compared to FGSM and BIM, significantly failing to capture malicious frames with ASR increasing from near-zero under FGSM/BIM to above 0.5 in many cases, reaching as high as 0.95 under same model. These observations are consistent with prior work showing that gradient-based adversarial methods can effectively exploit the differentiable decision boundaries of learning-based models [18], [23], [28].

In contrast, the ET model demonstrates comparatively higher robustness across most attack types, achieving notably lower ASR values. Although ET and RF perform similarly under FGSM and BIM, ET shows more stable missed-attack robustness under PGD, with lower and more gradual ASR increases than RF across all scenarios. However, all the models including ET remain vulnerable in the RLOFFA scenario, where ASR exceeds 0.43. For the FA dataset specifically, all models exhibit relatively low ASR, indicating greater resilience to missed attacks in this setting.

#### D. Gradient-Based and Protocol-Aware Vulnerabilities

The results show that gradient-based attacks (FGSM, BIM, and PGD) are highly effective against models that are directly or indirectly exploitable to gradient-based perturbations, including DNN leading to complete evasion in specific cases. This behavior is consistent with prior findings demonstrating that gradient-sign-based perturbations can induce high-confidence misclassification in DL models [18], [23].

In contrast, protocol-aware CAN fabrication attacks that manipulate the semantic content of payloads, such as MSA,

RLOFFA, and RLONA, have a stronger impact on tree-based models. While ET typically attains lower ASR than the other shallow models, DT, RF and XGB can attain significantly higher ASR, even approach near-complete evasion in missed-detections isolated cases (especially for PGD), exceeding ASR of 0.90. These results align with earlier observations that ensemble-based methods can reduce, but not fully eliminate, adversarial vulnerabilities in tree-based learners [33].

#### E. Comparative Robustness Across Models

Overall, most models remain robust to benign perturbations, as reflected by low false-positive ASR, but are substantially more vulnerable to adversarial manipulation of malicious samples. Although the DNN achieves superior benign robustness, it exhibits scenario-dependent catastrophic missed-attack behavior, reaching missed-attack ASR = 1.0 in adversarial settings, whereas ET maintains bounded in ASR (generally below 0.6) across all evaluated scenarios, resulting in more consistent missed-attack robustness overall. Thus, ET demonstrates the most favorable robustness trade-off, exhibiting minimal false alarms and comparatively lower missed-attack rates. These findings underscore the importance of adversarial evaluation for automotive IDS and motivate the use of robustness-oriented training strategies to improve resilience [15], [28].

The CSA attack does not produce any false negatives during adversarial evaluation. This outcome follows directly from the protocol-level constraints imposed during adversarial sample generation [4], [24], [34]. Perturbations are restricted to the eight data bytes, while CAN ID and DLC fields remain fixed and all modified values are clipped to the valid range [0, 255]. Frames violating these constraints are discarded to preserve CAN-frame validity. Consequently, no valid adversarial CSA samples reach the IDS, and no false-negative results are reported for this attack type.

## V. CONCLUSION

This work presents a systematic adversarial evaluation of in-vehicle IDS models operating on the CAN bus using the ROAD dataset. By analyzing both shallow and DL classifiers, we assess how different model architectures respond to constrained and realistic adversarial perturbations. The results reveal clear differences in robustness: Despite the DNN performing best on benign traffic, gradient-based attacks including FGSM, BIM, and PGD fully compromise the DNN-based IDS in terms of missed attacks under specific scenarios, whereas ensemble models, particularly ET, exhibit comparatively stronger resilience. These findings indicate that although neural models can capture complex feature relationships, they are highly susceptible to gradient-driven adversarial manipulation. Moreover, enforcing strict CAN domain constraints by limiting perturbations to valid payload bytes demonstrates that adversarial attacks can remain protocol-compliant and stealthy, underscoring their practical feasibility.

Overall, our results highlight the importance of adversarial robustness evaluation in automotive cybersecurity research. Future work will explore defense strategies such as adversar-

ial training, input sanitization, and hybrid IDS designs that combine learned representations with interpretable structures. As vehicles continue to advance toward greater autonomy and connectivity, ensuring that IDS solutions remain robust against adaptive adversaries will be critical for securing next-generation intelligent transportation systems.

#### ACKNOWLEDGMENT

This manuscript has been authored by UT-Battelle, LLC under Contract No. DE-AC05-00OR22725 with the U.S. Department of Energy. The publisher, by accepting the article for publication, acknowledges that the U.S. Government retains a non-exclusive, paid-up, irrevocable, worldwide license to publish or reproduce the published form of the manuscript, or allow others to do so, for U.S. Government purposes. The DOE will provide public access to these results in accordance with the DOE Public Access Plan. There was no additional external funding received for this study. The funders had no role in study design, data collection and analysis, decision to publish, or preparation of this manuscript. (<http://energy.gov/downloads/doe-public-access-plan>). This research was sponsored in part by Oak Ridge National Laboratory's (ORNL's) Laboratory Directed Research and Development program.

#### REFERENCES

- [1] A. B. C. Douss, R. Abassi, and D. Sauveron, "State-of-the-art survey of in-vehicle protocols and automotive ethernet security and vulnerabilities," *Math Biosci Eng*, vol. 20, no. 9, pp. 17057–17095, 2023.
- [2] W. Wu, R. Li, G. Xie, J. An, Y. Bai, J. Zhou, and K. Li, "A survey of intrusion detection for in-vehicle networks," *IEEE trans Intell Transp Syst*, vol. 21, no. 3, pp. 919–933, 2020.
- [3] W. Zeng, M. A. S. Khalid, and S. Chowdhury, "In-vehicle networks outlook: Achievements and challenges," *IEEE Communications Surveys & Tutorials*, vol. 18, no. 3, pp. 1552–1571, 2016.
- [4] S.-F. Lokman, A. T. Othman, and M.-H. Abu-Bakar, "Intrusion detection system for automotive controller area network (can) bus system: a review," *EURASIP J Wirel Commun Netw*, vol. 2019, no. 1, pp. 1–17, 2019.
- [5] H. J. Jo and W. Choi, "A survey of attacks on controller area networks and corresponding countermeasures," *IEEE trans Intell Transp Syst*, vol. 23, no. 7, pp. 6123–6141, 2022.
- [6] S. Checkoway, D. McCoy, B. Kantor, D. Anderson, H. Shacham, S. Savage, K. Koscher, A. Czeskis, F. Roesner, and T. Kohno, "Comprehensive experimental analyses of automotive attack surfaces," in *20th USENIX security symposium (USENIX Security 11)*, 2011.
- [7] K. Koscher, A. Czeskis, F. Roesner, S. Patel, T. Kohno, S. Checkoway, D. McCoy, B. Kantor, D. Anderson, H. Shacham *et al.*, "Experimental security analysis of a modern automobile," in *2010 IEEE symposium on security and privacy*. IEEE, 2010, pp. 447–462.
- [8] C. Miller and C. Valasek, "Remote exploitation of an unaltered passenger vehicle," *Black Hat USA*, vol. 2015, no. S 91, pp. 1–91, 2015.
- [9] M. Müter, A. Groll, and F. C. Freiling, "A structured approach to anomaly detection for in-vehicle networks," *2010 Sixth International Conference on Information Assurance and Security*, pp. 92–98, 2010.
- [10] S. Jin, J.-G. Chung, and Y. Xu, "Signature-based intrusion detection system (ids) for in-vehicle can bus network," in *2021 IEEE International Symposium on Circuits and Systems (ISCAS)*, 2021, pp. 1–5.
- [11] A. Faroughi and R. Javidan, "Canf: Clustering and anomaly detection method using nearest and farthest neighbor," *Future Gener Comput Syst*, vol. 89, pp. 166–177, 2018.
- [12] M. H. Shahriar, Y. Xiao, P. Moriano, W. Lou, and Y. T. Hou, "Canshield: deep-learning-based intrusion detection framework for controller area networks at the signal level," *IEEE Internet Things J*, vol. 10, no. 24, pp. 22 111–22 127, 2023.
- [13] W. Marfo, P. Moriano, D. K. Tosh, and S. V. Moore, "Detecting masquerade attacks in controller area networks using graph machine learning," *IEEE Trans Inf Forensics Secur*, vol. 20, pp. 13 127–13 142, 2025.
- [14] A. Alotaibi and M. A. Rassam, "Adversarial machine learning attacks against intrusion detection systems: A survey on strategies and defense," *Future Internet*, vol. 15, no. 2, 2023.
- [15] K. He, D. D. Kim, and M. R. Asghar, "Adversarial machine learning for network intrusion detection systems: A comprehensive survey," *IEEE Communications Surveys & Tutorials*, vol. 25, no. 1, pp. 538–566, 2023.
- [16] F. Aloraini and A. Javed, "Adversarial attacks in intrusion detection systems: triggering false alarms in connected and autonomous vehicles," in *2024 IEEE International Conference on Cyber Security and Resilience (CSR)*. IEEE, 2024, pp. 714–719.
- [17] S. Longari, F. Noseda, M. Carminati, and S. Zanero, "Evaluating the robustness of automotive intrusion detection systems against evasion attacks," in *International Symposium on Cyber Security, Cryptology, and Machine Learning*. Springer, 2023, pp. 337–352.
- [18] I. J. Goodfellow, J. Shlens, and C. Szegedy, "Explaining and harnessing adversarial examples," *International Conference on Learning Representations (ICLR)*, 2015.
- [19] M. E. Verma, R. A. Bridges, M. D. Iannacone, S. C. Hollifield, P. Moriano, S. C. Hespeler, B. Kay, and F. L. Combs, "A comprehensive guide to can ids data and introduction of the road dataset," *PLOS ONE*, vol. 19, no. 1, p. e0296879, 2024.
- [20] N. Hossain, "ADV\_ATTACKS\_ROAD\_CAN\_IVN\_IDS," [https://github.com/NirabHossain/ADV\\_ATTACKS\\_ROAD\\_CAN\\_IVN\\_IDS](https://github.com/NirabHossain/ADV_ATTACKS_ROAD_CAN_IVN_IDS), 2025, GitHub repository, accessed 22 Dec 2025.
- [21] D. Blevins, P. Moriano Salazar, R. Bridges, M. Verma, M. Iannacone, and S. Hollifield, "Time-based can intrusion detection benchmark," in *Proceedings of AutoSec 2021 – Third International Workshop on Automotive and Autonomous Vehicle Security*. Oak Ridge National Laboratory (ORNL), Oak Ridge, TN (United States), 01 2021.
- [22] H. Sun, M. Chen, J. Weng, Z. Liu, and G. Geng, "Anomaly detection for in-vehicle network using cnn-lstm with attention mechanism," *IEEE Trans Veh Technol*, vol. 70, no. 10, pp. 10 880–10 893, 2021.
- [23] N. Carlini and D. Wagner, "Towards evaluating the robustness of neural networks," in *IEEE Symposium on Security and Privacy (SP)*, 2017, pp. 39–57.
- [24] F. Luo, J. Wang, X. Zhang, Y. Jiang, Z. Li, and C. Luo, "In-vehicle network intrusion detection systems: a systematic survey of deep learning-based approaches," *PeerJ Comput Sci*, vol. 9, p. e1648, 2023.
- [25] Y. Pacheco and W. Sun, "Adversarial machine learning: A comparative study on contemporary intrusion detection datasets," in *ICISSP*, 2021, pp. 160–171.
- [26] I. Zenden, H. Wang, A. Iacovazzi, A. Vahidi, R. Blom, and S. Raza, "On the resilience of machine learning-based ids for automotive networks," in *2023 IEEE Vehicular Networking Conference (VNC)*. IEEE, 2023, pp. 239–246.
- [27] P. Moriano, S. C. Hespeler, M. Li, and R. A. Bridges, "Evaluating lightweight unsupervised online ids for masquerade attacks in can," *arXiv preprint arXiv:2406.13778*, 2025.
- [28] M.-I. Nicolae, M. Sinn, M.-N. Tran, B. Bueser, A. Rawat, M. Wistuba, V. Zantedeschi, N. Baracaldo, B. Chen, H. Ludwig, I. Molloy, and B. Edwards, "Adversarial robustness toolbox v1.0.0," *arXiv: Learning*, 2018. [Online]. Available: <https://api.semanticscholar.org/CorpusID:219890559>
- [29] A. Kurakin, I. Goodfellow, and S. Bengio, "Adversarial examples in the physical world," *arXiv preprint arXiv:1607.02533*, 2016.
- [30] A. Madry, A. Makelov, L. Schmidt, D. Tsipras, and A. Vladu, "Towards deep learning models resistant to adversarial attacks," in *International Conference on Learning Representations (ICLR)*, 2018.
- [31] Y. Li, L. Li, L. Wang, T. Zhang, and B. Gong, "Nattack: Learning the distributions of adversarial examples for an improved black-box attack on deep neural networks," in *International conference on machine learning*. PMLR, 2019, pp. 3866–3876.
- [32] D. Chicco and G. Jurman, "The advantages of the matthews correlation coefficient (mcc) over f1 score and accuracy in binary classification evaluation," *BMC genomics*, vol. 21, no. 1, p. 6, 2020.
- [33] N. Papernot, P. McDaniel, and I. Goodfellow, "Transferability in machine learning: from phenomena to black-box attacks using adversarial samples," *arXiv preprint arXiv:1605.07277*, 2016.
- [34] A. Wasicek, M. D. Pesé, A. Weimerskirch, Y. Burakova, and K. Singh, "Context-aware intrusion detection in automotive control systems," in *Proc. 5th ESCAR USA Conf*, 2017, pp. 21–22.